Journal of Power Sources 196 (2011) 8802–8808

Contents lists available at ScienceDirect

Journal of Power Sources

journal homepage: www.elsevier.com/locate/jpowsour

Effect of iron doped lead oxide on the performance of lead acid batteries

Jianwen Liu, Danni Yang, Linxia Gao, Xinfeng Zhu, Lei Li, Jiakuan Yang*

School of Environmental Science and Engineering, Huazhong University of Science and Technology (HUST), Wuhan 430074, PR China

ARTICLE INFO

Article history:
Received 22 March 2011
Received in revised form 22 June 2011
Accepted 23 June 2011
Available online 30 June 2011

Keywords:
Lead acid battery
Iron
Lead oxide
Battery capacity
Battery cycle life
Release of hydrogen and oxygen

ABSTRACT

In order to investigate effect of iron on the performance of lead acid batteries, we systematically study the chemical characteristics, electrochemical characteristics, battery capacity and cycle life using iron-doped lead oxide in this article. Cyclic voltammetry results show that positive discharge current decreases sharply with the increasing content of Fe_2O_3 from 0.05 wt.% to 2 wt.%. The release of H_2 and O_2 are promoted accompanying the increase of Fe_2O_3 contents. The chemical analysis confirms that the strength of Fe^{3+}, Fe^{2+} concentration is simultaneously increased with the increase of iron contents after 50 voltammetry cycles. X-ray diffraction phase analysis shows that the amount of $PbSO_4$ increases with the increasing iron content in the positive plates after 50 discharge cycles. Morphologies of positive plates show that many agglomerates from $PbSO_4$ crystals appear. The SEM observations illustrate that there is a lower porosity and specific surface area in the positive active material with iron after 50 discharge cycles. The mechanism of iron decreasing capacity, cycle-life and promoting the release of H_2 and O_2 has been elucidated in details. We support it is the "redox-diffusion" process of multiple-valence iron and formation of $PbSO_4$ on electrodes that result in above performances.

1. Introduction

Presently traditional preparation of lead oxide is based on crude lead and refining lead from the pyrometallurgical process, which produces pure lead oxide because of smelting and refining at high temperature. However due to high energy consumption and large emission of volatile lead dust and SO_2, the pyrometallurgical process needs to be replaced with sustainable and environmental-friendly process. Nowadays utilization rate of secondary lead is gradually rising in total lead resources. The metallurgy of secondary lead is mainly derived from waste lead acid batteries. Therefore many researchers have developed various hydrometallurgical processes for preparation of secondary lead resource or lead oxides from spent batteries, which significantly reduce much energy consumption than conventional pyrometallurgical process. In recent years Prengamann and McDonald [1] invented a process of $(NH_4)_2CO_3$–Na_2SO_3–H_2SiF_4 hydro-electric-deposition for lead recovery from waste lead pastes. Chen [2] developed this process with a Na_2CO_3–H_2O_2–HBF_4/H_2SiF_4 hydro-electric-deposition. Kumar and Sonmez [3,4] used citrate and sodium citrate to leach out lead citrate from spent lead acid battery pastes; then received lead citrate was calcinated at a low temperature of 325 °C to prepare lead oxide directly. Karami et al. [5,6] investigated the synthesis of nano-structured lead oxide through reaction of lead nitrate solution and sodium carbonate solution by a sono-chemical method.

However hydrometallurgical process can inevitably bring some impurity elements in final lead oxides due to liquid-phase reaction and waste-battery origin [1–7]. The role and mechanism of impurity elements in lead oxide has been studied by CSIRO and Pasminco Metals [8–12]. Dr. Lam studied the influence of around 17 different elements in lead oxide on the VRLA battery performance [13]. Prengamann evaluated the effects of many different impurities (including Ag, Bi, Zn, Sn, Sb) on the hydrogen and oxygen evolution currents at different temperatures and potentials [14]. Rice and Manders observed that bismuth in lead oxide was the promotion of efficient oxygen recombination in VRLA batteries [15]. Pavlov et al. found that carbon can increase the specific surface area of negative active materials and promote the applicability of lead acid battery in hybrid electric vehicles [16]. In China researchers have tried to test the influence of impurity elements doped lead oxide on the performance of lead acid batteries. Chen and co-workers analyzed the effects of Bi-doped lead oxides in the lead acid battery [17]. Liu et al. investigated the harm of iron in lead acid battery [18]. Zhou et al. proved that Sb can increase discharge capacity and utilization rate of active materials of lead acid batteries [19]. Feng et al. analyzed the effect and mechanism of Bi and Sn on the battery performance [20].

These research results above have no systematical significance for novel ultra-fine lead oxide because of the distinctiveness of hydrometallurgical process. However it is very important for us to study the effect of impurity elements doped lead oxide in

* Corresponding author. Tel.: +86 27 87792207; fax: +86 27 87792101.
E-mail addresses: jkyang@mail.hust.edu.cn, yjiakuan@hotmail.com (J. Yang).

0378-7753/$ – see front matter © 2011 Elsevier B.V. All rights reserved.
doi:10.1016/j.jpowsour.2011.06.084

lead acid batteries accompanying the invention of hydrometallurgical process. Iron is a kind of common impurity in battery, and it plays a key role on battery performance. Therefore the effect of iron was studied first in this article. We investigate the performance from chemical characteristics, electrochemical characteristics, and battery performance using iron doped lead oxide. The X-ray diffraction (XRD), scanning electron microscope (SEM), cyclic voltammetry (CV), electrochemical impedance spectroscopy (EIS), chemical analysis and battery test method were used to analyze these performances.

2. Experimental

2.1. Chemicals

Lead oxide was provided by Wuhan Changguang Power Sources Cooperation Limited of China. The lead oxide comprised approximately 75% of PbO and 25% of Pb. Fe_2O_3 (impurity ≥99.9%) in the experiment was purchased from Sinopharm Chemical Reagent Cooperation Limited of China.

2.2. Electrochemical test

2.2.1. Electrode preparation

The seven kinds of lead oxide doped with different iron contents were prepared from mechanical mixing and ball-mill process. They were presented as follows:

(1) pure lead oxide;
(2) lead oxide doped with 0.01 wt.% Fe_2O_3;
(3) lead oxide doped with 0.05 wt.% Fe_2O_3;
(4) lead oxide doped with 0.1 wt.% Fe_2O_3;
(5) lead oxide doped with 0.5 wt.% Fe_2O_3;
(6) lead oxide doped with 1 wt.% Fe_2O_3;
(7) lead oxide doped with 2 wt.% Fe_2O_3.

The outer surface of electrode containing with active material above was a square of 10 mm × 10 mm.

2.2.2. Electrochemical test

The cyclic voltammetry (CV) method was applied to observe the change of electrochemical behavior with iron or without iron over a certain voltage range. The CV curves were tested by three electrode system. The positive active material prepared from different lead oxides was used as the working electrode (10 mm × 10 mm). The counter electrode was double platinum electrode, and the reference electrode was an $Hg/Hg_2SO_4/K_2SO_4$ (sat.) electrode. The electrolyte was sulfuric acid solution (3 mol L^{-1}). All experiments were performed at room temperature using a VMP-2 device from USA. In every experiment current and voltage curves of fifth cycle were recorded as final results with a scanning speed of 20 mV s^{-1}.

The EIS was tested by the same VMP-2 device. The EIS curves were recorded with a frequency from 0.1 Hz to 100 kHz.

2.3. Chemical analysis

The electrolytes taken for chemical analysis included sulfuric acid solution before iron soaking, sulfuric acid solution after iron soaking and sulfuric acid solution after cyclic voltammetry (50 cycles). The pH value and Fe^{3+}, Fe^{2+} ion concentration were tested and analyzed by a pH testing meter and atomic absorption spectroscopy (AAS) method respectively.

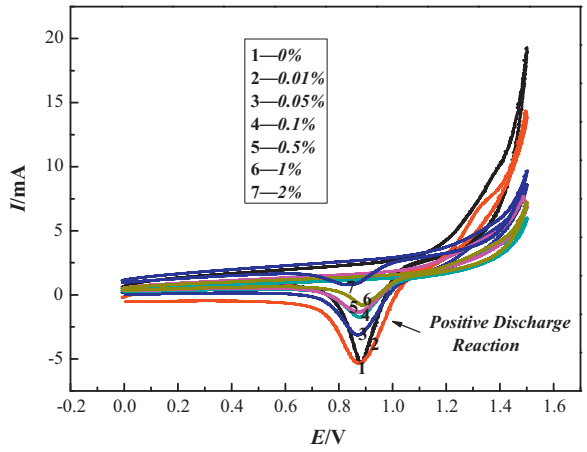

Fig. 1. Cyclic voltammetry curves of Fe-free and Fe-doped positive electrodes: lead oxide being doped 0.00, 0.01, 0.05, 0.1, 0.5, 1, and 2 wt.% Fe_2O_3.

2.4. Characterization of positive active materials

The morphology of the positive active-material was examined by ESEM Quanta-200FEG FEI scanning electron microscopy (SEM) technique.

The phase composition of the positive active-material was determined by X-ray diffraction (XRD) phase-analysis by D/MAX 2550 X-ray diffraction analyzer (from Japan) using Cu K_α radiation (λ = 1.54 Å) at 300 mA and 40 kV.

2.5. Battery test

2.5.1. Battery manufacture

The lead oxide was made in the same Chinese factory. With the same technical process for oxide, paste-mixing, paste-curing, formation, washing and drying treatment, the different positive and negative plates were produced.

The grids were low antimony alloys of Sn–Al–Ca–Pb: Sn 0.28–0.32 wt.%, Al 0.015–0.020 wt.%, Ca 0.09–0.10 wt.%.

The polyethylene pocket separators were inserted and sulfuric acid solution (1.250 relative density) was used as electrolyte.

2.5.2. Performance test

Different types of plates prepared from different lead oxides were assembled in batteries (2 V/2 Ah). The performance was tested according to the Chinese National Standard (GB5008.1-91).

3. Results

3.1. Electrochemical results

3.1.1. CV results

Fig. 1 shows CV curves with and without iron oxides in the potential range of 0.5–1.2 V. Peak in this range reveals positive discharge reaction of lead acid battery, and corresponding reaction is shown in Eq. (1):

$$PbO_2 + HSO_4^- + 3H^+ + 2e^- \rightarrow PbSO_4 + 2H_2O \quad (1)$$

These results clearly state that content of Fe_2O_3 below 0.05 wt.% in the positive active material does not affect the electrochemical behavior of positive discharge reaction. When Fe_2O_3 content increases from 0.05 wt.% to 2 wt.%, positive discharge current decreases significantly. No other reductive peaks or oxidative peaks are observed, and the peak potential does not shift. Corresponding variation trend of positive discharge current at different Fe_2O_3 contents is shown in Fig. 2.

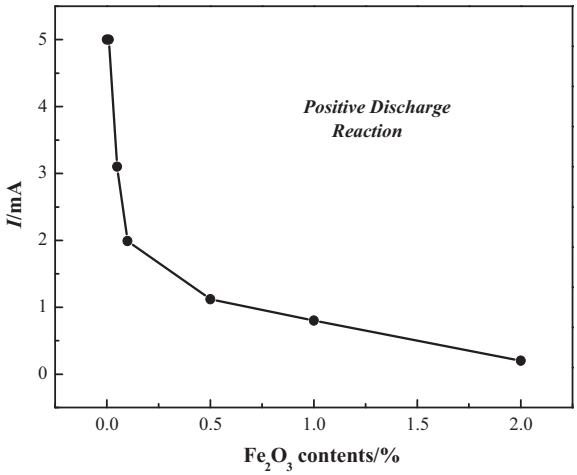

Fig. 2. Variation trend of positive discharge current at different Fe_2O_3 contents: lead oxide being doped 0.00, 0.01, 0.05, 0.1, 0.5, 1, and 2 wt.% Fe_2O_3.

Fig. 3 shows CV curves of different Fe_2O_3 contents within −1.4 V to 0 V. Peak in this range reveals negative discharge reaction of lead acid battery, and corresponding reaction is shown in Eq. (2):

$$Pb + HSO_4^- - 2e^- = PbSO_4 + H^+ \quad (2)$$

The presence of iron in the negative active material does not affect the electrochemical behavior of negative discharge reaction. No other reductive peaks or oxidative peaks are seen, and the peak potential does not shift significantly.

Whereas, Fig. 4(a) and (b) shows distinct peak evolution in CV curves due to O_2 and H_2-release reaction within 1.0–1.8 V and −1.2 to −0.7 V respectively at different Fe_2O_3 contents. Corresponding reaction is shown in Eqs. (3) and (4):

$$2H_2O = 4H^+ + 4e^- + O_2 \quad (3)$$

$$2H^+ + 2e^- = H_2 \quad (4)$$

It can be easily observed that the release of H_2 and O_2 are promoted accompanying the increase of Fe_2O_3 contents, which does obvious disadvantage on performance of lead acid batteries.

3.1.2. EIS results

The electrochemical impedance spectroscopy reflects interface properties of battery performance. The more the Re (Z), the higher the battery impedance. Variation trend of Re (Z) at different Fe_2O_3 contents is shown in Fig. 5. The impedance in battery system is increased with the increase of Fe_2O_3 contents.

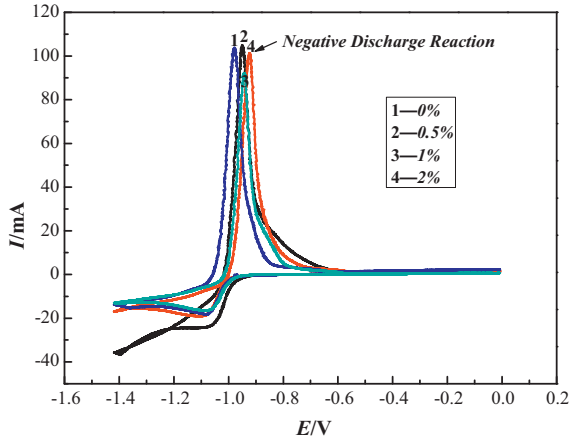

Fig. 3. Cyclic voltammetry curves of Fe-free and Fe-doped negative electrodes: lead oxide being doped 0.00, 0.05, 0.5, and 1 wt.% Fe_2O_3.

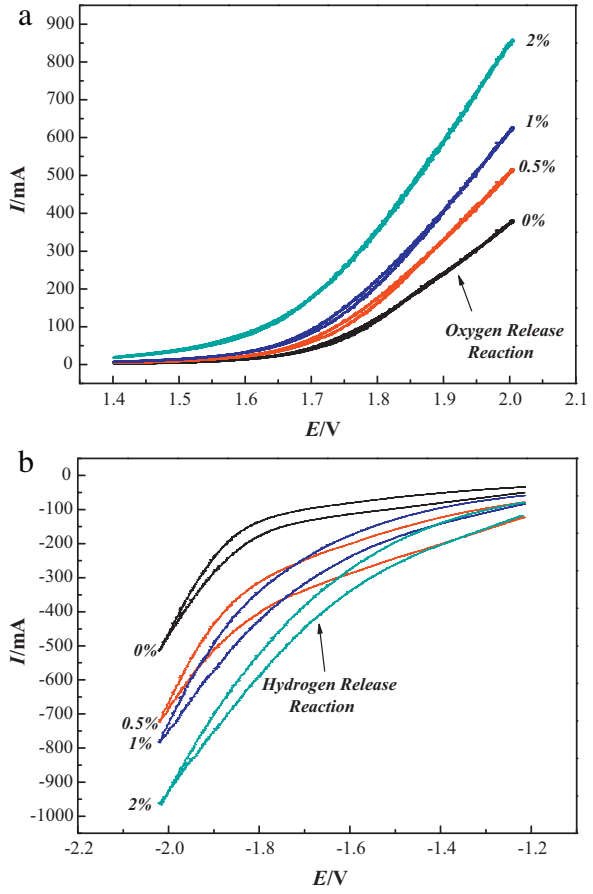

Fig. 4. (a) Cyclic voltammetry curves of O_2 release reaction: lead oxide being doped 0.00, 0.5, 1.0 and 2 wt.% Fe_2O_3. (b) Cyclic voltammetry curves of H_2 release reaction: lead oxide being doped 0.00, 0.5, 1.0 and 2.0 wt.% Fe_2O_3.

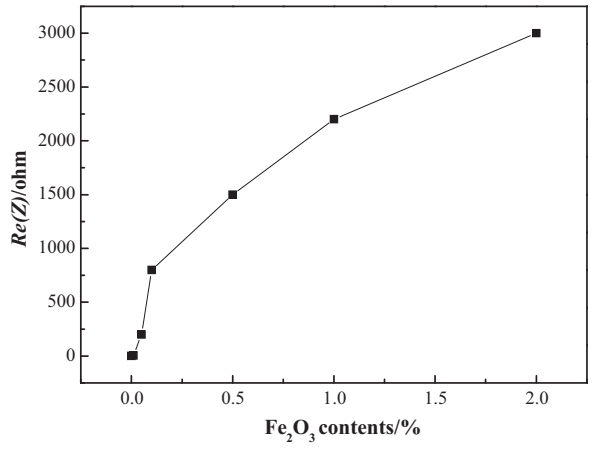

Fig. 5. Variation trend of Re (Z) at different Fe_2O_3 contents: lead oxide being doped 0.00, 0.01, 0.05, 0.1, 0.5, 1, 2 wt.% Fe_2O_3.

3.2. Results of chemical analysis for electrolyte

In order to monitor the change of H^+, Fe^{3+}, Fe^{2+} concentration in the electrolyte, chemical analysis for electrolyte was performed. The positive and negative plates were made from lead oxide doped

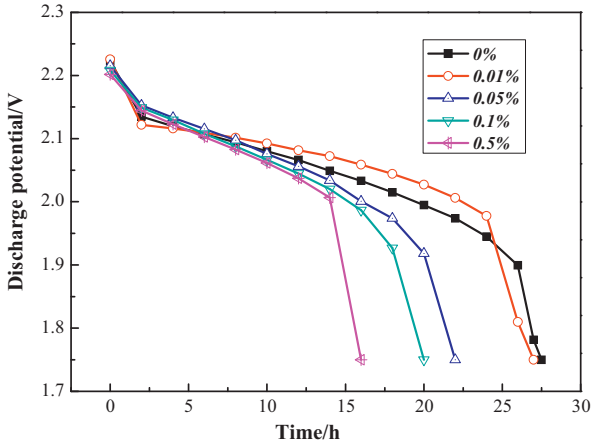

Fig. 6. The 20 h rate curve of batteries manufactured by lead oxide doped with 0.00, 0.01, 0.05, 0.1, and 0.5 wt.% Fe_2O_3.

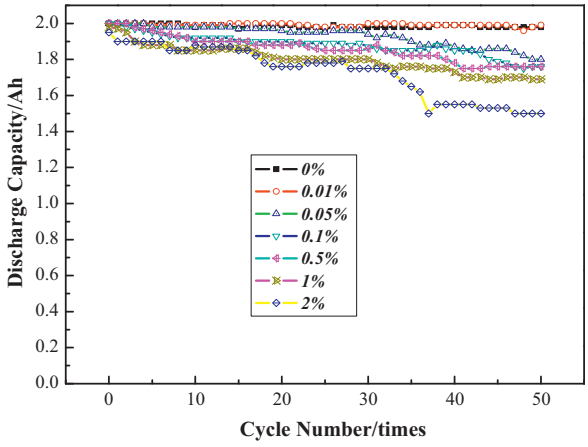

Fig. 7. Cycle performance of batteries manufactured by lead oxide doped with 0.00, 0.01, 0.05, 0.1, 0.5, 1, 2 wt.% Fe_2O_3.

with 0.01, 0.05, 0.1, 0.5, 1 wt.% Fe_2O_3. The electrolytes were prepared as follows:

(1) Sulfuric acid solution (1.12 g L^{-1}) with plates soaked for 2 h.
(2) Sulfuric acid solution (1.28 g L^{-1}) after 50 voltammetry cycles of the positive plates.
(3) Sulfuric acid solution (1.28 g L^{-1}) after 50 voltammetry cycles of the negative plates.

The results of chemical analysis for ion concentration in the electrolyte are given in Table 1.

The concentration of Fe^{3+}, Fe^{2+} in the sulfuric acid solution is too low when only electrode plate soaked, while it is significantly increased after 50 voltammetry cycles. The strength of Fe^{3+}, Fe^{2+} concentration is simultaneously increased with the increase of iron concentration.

However, no obvious change of pH value in the electrolyte appears.

3.3. Results of battery performance

In this experiment, 2 Ah battery was manufactured by lead oxide doped with 0.00, 0.01, 0.05, 0.1, 0.5 wt.% Fe_2O_3. Battery performance was tested according to the experimental methods of the Chinese National Standard.

The 20 h rate was tested with a discharge current of 100 mA. The results of battery performance were shown in Fig. 6. First, no obvious difference between Fe-free plates and 0.01 wt.% Fe-doped plates is found in Fig. 6. While the 20 h rate is sharply decreased when Fe_2O_3 content increases from 0.05 wt.% to 0.5 wt.%. The results of 20 h rate are similar to electrochemical results in Section 3.1.1.

Meanwhile cycle performance of batteries manufactured by lead oxide doped with 0.00, 0.01, 0.05, 0.1, 0.5, 1, 2 wt.% Fe_2O_3 is shown in Fig. 7. First cycle performance of 0.01 wt.% Fe-doped battery is the same as that of Fe-free battery. While cycle performance of 0.05 wt.% Fe-doped battery after 50 numbers is below 90% of standard performance, that of 0.5 wt.% Fe-doped battery after 50 cycles is even below 70% of standard performance, which is far below standard demand in practical use. The results of cycle performance are also similar to electrochemical results in Section 3.1.1.

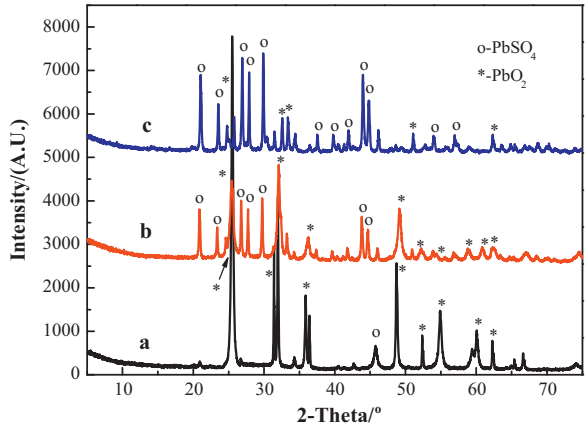

Fig. 8. XRD patterns of the positive active materials after 50 discharge cycles: (a) Fe-free battery; (b) 0.05 wt.% Fe-doped battery and (c) 0.5 wt.% Fe-doped battery.

3.4. SEM images and XRD results

The phase composition of the positive active material after 50 discharge cycles was determined by X-ray diffraction (XRD) phase analysis. XRD results are shown in Fig. 8. Obviously the amount of $PbSO_4$ increases with the increasing iron content in the positive plates after 50 discharge cycles. The related quantitative results are reported in Table 2.

Table 1
Chemical analysis for ion concentration in the electrolyte.

Electrolyte type	Positive plates with iron					Negative plates with iron				
	0.01%	0.05%	0.1%	0.5%	1%	0.01%	0.05%	0.1%	0.5%	1%
H_2SO_4 with plate soaking	–	–	–	+[a]	+[a]	–	–	–	+[b]	+[b]
H_2SO_4 after 50 voltammetry cycles	+[a]	++[a]	++++[a]	++++[a]	+++++[a]	+[b]	++[b]	+++[b]	+++[b]	++++[b]

[a] The more symbol "+", the higher Fe^{3+} ion concentration.
[b] The more symbol "+", the higher Fe^{2+} ion concentration.

Table 2
Quantitative results of crystalline phase in the positive active material after 50 discharge cycles (wt.%).

Phases	Positive active materials made with pure lead oxide (Fe-free)	Positive active materials made with lead oxide doped with 0.05 wt.% Fe_2O_3	Positive active materials made with lead oxide doped with 0.5 wt.% Fe_2O_3
PbO_2	96.52	54.03	36.26
$PbSO_4$	1.68	44.66	62.74
Other phase	1.80	1.31	1.00

Morphologies of the positive active materials after 50 discharge cycles are shown in Fig. 9. In Fig. 9(a) the structure of PbO_2 is loose and porous. While in Fig. 9(b) and (c) many agglomerates from $PbSO_4$ crystals appear. The SEM observations illustrate that there is a lower porosity and specific surface area in the positive active material with iron after 50 discharge cycles.

4. Discussion

4.1. Chemical characteristics of iron in the battery plate

To discuss the mechanism of iron oxide on lead acid battery, it is prerequisite to know the exact phases and oxides of iron as impurity. In general oxides of iron exist in five forms: FeO, Fe_3O_4, Fe_2O_3, FeO_2, FeO_3. Among them, an alkaline Fe_2O_3 is most-stable and can be easily dissolved in acid. In the solution, the form of iron existing is Fe^{3+} ion or hydrated FeO^+ ion.

In this experiment, chemical reactions about Fe_2O_3-doped lead oxide initially took place in H_2SO_4 solution during paste-mixing and curing process. Thus the form of iron existing in the Fe_2O_3–SO_3–H_2O system has been investigated. The stable and basic compounds in the Fe_2O_3–SO_3–H_2O system have been listed as follows [21]:

$Fe_2(SO_4)_3$, $Fe_2(SO_4)_3{\cdot}9H_2O$, $Fe_2(SO_4)_3{\cdot}nH_2O$, $FeH(SO_4)_2$, $FeH(SO_4)_2{\cdot}nH_2O$, $Fe_3H(SO_4)_5$, $Fe_3H(SO_4)_5{\cdot}nH_2O$, $Fe(OH)_3$, $Fe(OH)SO_4$, $Fe(OH)SO_4{\cdot}nH_2O$, (FeO)OH, $(FeO)SO_4$, $(FeO)SO_4{\cdot}nH_2O$.

Among them for example, the usual chemical reaction product of iron in the sulfuric acid is $Fe_2(SO_4)_3$, the hydrolysis product of $Fe_2(SO_4)_3$ probably includes $Fe(OH)_3$, $Fe(OH)SO_4$, (FeO)OH, etc.

The above compounds of iron are the products of chemical reactions without any voltage effects. The electrochemical characteristics are discussed in Section 4.2.

4.2. Electrochemical reactions of iron in the battery plate

When iron is used in electrodes of batteries, its chemical reactions get influenced by the voltage. In order to know the change of iron forms and its influence on the electrodes, we use the Pourbaix diagram of the Fe–H_2O system (shown in Fig. 10) to analyze the electrochemical reactions of iron in positive plates referenced to pH value [22].

According to our discussion in Section 4.1, $Fe_2(SO_4)_3$, $Fe(OH)_3$, $Fe(OH)SO_4$, (FeO)OH, $FeH(SO_4)_2$ may be the main existing forms of iron when Fe_2O_3 is reacted with sulfuric acid during paste-mixing and curing process. Besides, other soluble salt of iron may also be produced.

During the charge–discharge and cycling processes, the possible existing forms of iron include: $Fe(OH)_2$, $Fe(OH)_3$, Fe^{3+}, Fe^{2+}, $Fe(OH)^{2+}$, $FeOH^+$, $FeOOH^-$, FeOOH, etc. from Fig. 10. The electro-

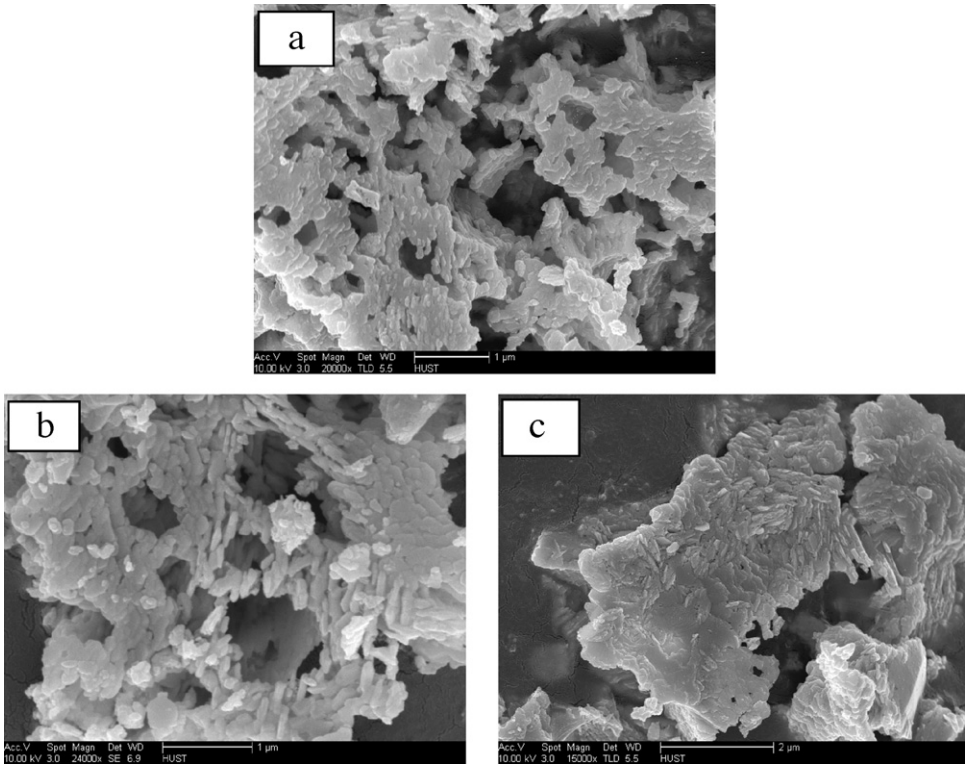

Fig. 9. SEM morphology of the positive active materials after 50 discharge cycles: (a) Fe-free battery; (b) 0.05 wt.% Fe-doped battery and (c) 0.5 wt.% Fe-doped battery.

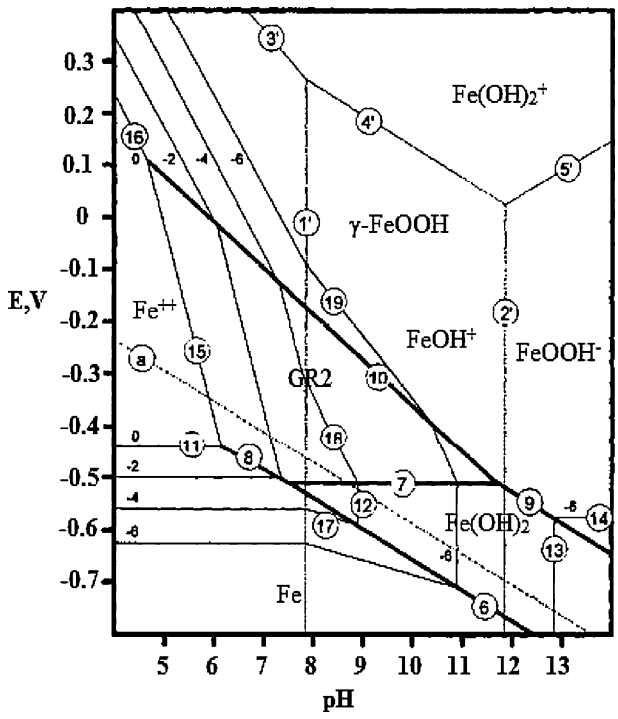

Fig. 10. E vs pH Pourbaix diagram of iron in sulphate-containing aqueous media.

chemical reactions among these compounds can be expressed in Eqs. (6)–(14):

$$Fe^{2+} + 2H_2O \rightarrow Fe(OH)^{2+} + 2H^+ + e^- \quad (6)$$

$$FeOH^+ + H_2O \rightarrow Fe(OH)^{2+} + H^+ + e^- \quad (7)$$

$$FeOOH^- + H^+ \rightarrow Fe(OH)^{2+} + e^- \quad (8)$$

$$Fe(OH)_2 \rightarrow FeOOH + H^+ + e^- \quad (9)$$

$$FeOOH^- \rightarrow FeOOH + e^- \quad (10)$$

$$Fe^{2+} + 2H_2O \rightarrow FeOOH + 3H^+ + e^- \quad (11)$$

$$Fe + H_2O \rightarrow FeOH^+ + H^+ + 2e^- \quad (12)$$

$$FeOH^+ + H_2O \rightarrow FeOOH + 2H^+ + e^- \quad (13)$$

$$Fe^{3+} + e^- \rightarrow Fe^{2+} \quad (14)$$

Through electrochemical reactions, oxides of iron in high valence states come into being at anode, while those of low valence appear at cathode. Chemical analysis in Section 3.2 indicates that some of iron passes into sulfuric acid, and its effects are discussed below.

4.3. Effect and mechanism of iron decreasing battery capacity and cycle-life

The working theory of lead acid battery can be demonstrated in Eqs. (1) and (2), and the total reaction in the electrode is shown in Eq. (15).

$$PbO_2 + Pb + 2H^+ + 2HSO_4^- \rightarrow PbSO_4 + 2H_2O \quad (15)$$

In Section 3.2, the results of chemical analysis confirm that a trace of Fe^{3+}, Fe^{2+} ion exists in the sulfuric acid solution during charge–discharge process and battery cycle.

In Section 3.4, XRD patterns of the positive active materials show that the increasing iron content results in an increase of $PbSO_4$ crystals, which is the irreversible product of battery cycling. $PbSO_4$ product does severe disadvantage for battery capacity and cycle-life.

In Section 3.4, the SEM morphology of the positive active materials shows that there are many agglomerates from $PbSO_4$ crystals. Moreover this phenomenon appears an increasing trend with the increase of iron, which directly leads to the lower porosity and specific surface area of the positive active material. Therefore agglomerates also do severe disadvantage for battery capacity and cycle-life.

In view of the foregoing, a microcell comes into being in the internal of battery system accompanying the impurity of iron transferring into the electrolyte. The multiple-valence iron can generate corrosion at electrodes, cause much loss of active materials, promote self-discharge.

Low-valence iron is oxidized and PbO_2 is simultaneously reduced at anode, and high-valence iron can be transferred to cathode through convection and diffusion. Then this high-valence iron is reduced and active Pb is simultaneously oxidized at cathode. Moreover this redox process will be repeatedly cycled because of ion convection and diffusion between two electrodes. The electrochemical reaction of microcell is stated as follows:

$$PbO_2 + 3H^+ + HSO_4^- + 2Fe^{2+} \rightarrow PbSO_4 + 2H_2O + 2Fe^{3+} \quad (16)$$

$$Pb + HSO_4^- + 2Fe^{3+} \rightarrow PbSO_4 + H^+ + 2Fe^{2+} \quad (17)$$

Therefore self-discharge will be continuously proceeded in the electrodes due to the existence of iron, which causes fatal effect for battery capacity.

Meanwhile, dense irreversible $PbSO_4$ crystals are produced and depleted on electrodes through repeatedly cycled redox process, which reduces cycle and overall performance of lead acid battery.

4.4. Effect and mechanism of iron promoting release of H_2 and O_2

In Section 3.1.1, the CV results show that impurity of iron can promote release of H_2 and O_2. Excessive release of H_2 and O_2 can cause much loss of water, which leads to poor battery performance.

We observed in Section 4.3, the multiple-valence iron coexists in the electrolyte through "redox-diffusion" process. It is this multiple-valence iron that promotes release of H_2 and O_2. The process can be stated by the following equations.

$$4Fe^{3+} + 2H_2O \rightarrow 4H^+ + O_2 + 4Fe^{2+} \quad (18)$$

$$2Fe^{2+} + 2H^+ \rightarrow H_2 + 2Fe^{3+} \quad (19)$$

5. Conclusions

At present it is very important for us to study the effect of iron doped lead oxide in lead acid batteries accompanying the invention of hydrometallurgical process for preparation of novel ultra-fine lead oxide. In this article we investigate the performance from the following 3 aspects: chemical characteristics, electrochemical characteristics, battery performance. We also discuss the effect and mechanism in details. The results prove that iron in lead oxide is a fatal element for lead acid batteries. High contents of iron over 0.05 wt.% in lead oxide can sharply decrease the battery capacity and cycle-life. Impurity of iron in lead oxide can promote the release of H_2 and O_2. These all do great harm for lead acid battery. Through discussion we support it is the "redox-diffusion" process of multiple-valence iron and formation of $PbSO_4$ on electrode that result in bad performances.

Acknowledgements

The authors thank for the financial supports from the National Science Council of China (NSC 50804017) and New Century Excel-

lent Talents Project of Ministry of Education (NCET-09-0392). The authors would like to thank the Analytical and Testing Center of Huazhong University of Science and Technology for providing the facilities to fulfill the experimental measurements. The technical supports from Wuhan Changguang Power Sources Co. Ltd., are also gratefully acknowledged.

References

[1] R.D. Prengamann, H.B. McDonald, US Patent 4,230,545 (1980).
[2] W.P. Chen, Journal of Hunan University in China 23 (1996) 111–116.
[3] M.S. Sonmez, R.V. Kumar, Hydrometallurgy 95 (2009) 53–60.
[4] M.S. Sonmez, R.V. Kumar, Hydrometallurgy 95 (2009) 82–86.
[5] H. Karami, M.A. Karami, S. Haghdar, Materials Research Bulletin 43 (2008) 3054–3065.
[6] H. Karami, M.A. Karami, S. Haghdar, A. Sedeghi, Materials Chemistry and Physics 108 (2008) 337–344.
[7] W.S. Li, X.M. Long, J.H. Yan, J.M. Nan, H.Y. Chen, Y.M. Wu, Journal of Power Sources 158 (2006) 1096–1101.
[8] L.T. Lam, N.P. High, O.V. Lim, D.A. Rand, J.E. Manders, Journal of Power Sources 78 (1999) 139–146.
[9] L.T. Lam, N.P. High, O.V. Lim, D.A. Rand, J.E. Manders, D.M. Rice, Journal of Power Sources 73 (1998) 36–46.
[10] L.T. Lam, J.D. Douglas, R. Pilling, D.A. Rand, Journal of Power Sources 48 (1994) 219–232.
[11] L.T. Lam, H. Ozgun, O.V. Lim, J.A. Hamilton, L.H. Vu, D.G. Vella, D.A. Rand, Journal of Power Sources 53 (1995) 215–228.
[12] L.T. Lam, N.P. High, C.G. Phyland, N.C. Wilson, D.G. Vella, L.H. Vu, D.A. Rand, J.E. Manders, C.S. Lakshmi, Proceedings of the INTELEC'98, San Fransico, USA, 1998, pp. 452–460.
[13] L.T. Lam, H. Ceylan, N.P. Haigh, T. Lwin, D.A. Rand, Journal of Power Sources 195 (2010) 4494–4512.
[14] R.D. Prengamann, Journal of Power Sources 144 (2005) 426–437.
[15] D.M. Rice, J.E. Manders, Journal of Power Sources 67 (1997) 251–255.
[16] D. Pavlov, P. Nikolov, T. Rogachev, Journal of Power Sources 196 (2011) 5155–5167.
[17] H.Y. Chen, L. Wu, C. Ren, Q.Z. Luo, Z.H. Xie, X. Jiang, S.P. Zhu, Y.K. Xia, Y.R. Luo, Journal of Power Sources 95 (2001) 108–118.
[18] Q. Liu, H. Liu, H.G. Shao, Lead Acid Battery 47 (2010) 162–165.
[19] Y. Zhou, P.X. Zu, Y. Sun, Power Technology 33 (2009) 291–294.
[20] W.H. Feng, G.Z. Zhang, Z.G. Zhang, Power Technology 23 (1999) 17–18.
[21] Gmelin Handbuch Der Anorganischen Chemie, System-NR.19, Wismut, 1964.
[22] X.Z. Yang, W. Yang, Electrochemical Thermodynamics of Metals Corrosion–Potential–pH Diagram and Application, Chemical Industry Press, Beijing, 1991.